

*stereolithography, numerical modelling,  
tensile test, resin*

*Danuta MIEDZIŃSKA* [0000-0003-2503-6600]\*, *Ewelina MAŁEK*,  
*Arkadiusz POPLAWSKI* [0000-0002-7494-8975]\*

## **NUMERICAL MODELLING OF RESINS USED IN STEREOLITOGRAPHY RAPID PROTOTYPING**

### **Abstract**

*The presented research deals with the development of the numerical model for resins used for stereolithography (SLA) rapid prototyping. SLA is an additive method of production of models, prototypes, elements or parts of constructions with the use of 3D printing that covers photochemical processes by which light causes chemical monomers to link together to form polymers. Such method is very useful in design visualization, but also can be applied in numerical modelling for the purpose of validation and verification. In this application the resin strength parameters must be described and on the base of them the numerical material model is developed and validated. Such a study for SLA resins was presented in the paper.*

### **1. INTRODUCTION – AIM OF RESEARCH**

Stereolithography is one of the methods of rapid prototyping. Models – prototypes – are made of a special photocurable resin. The curing of the resin takes place due to irradiation with a laser light of the appropriate wavelength. The accuracy of model mapping depends on many factors, including the geometric accuracy of the stereolithographic apparatus (Attaran, 2017; Melchels, Feijena & Grijpmaab, 2010; ISO/ASTM International Standard, 2015).

---

\* Military University of Technology, Faculty of Mechanical Engineering, Kaliskiego 2 St.,  
Warsaw, Poland

The initial model for the stereolithographic one is the solid created in the CAD system (Fig. 1a). The accuracy of the body depends on the CAD system used and the modeling method adopted, which is a separate issue. The finished CAD model is exported to the stereolithography format, often referred to as STL (from the file name extension) (Fig. 1b). This format describes each modeled solid by means of flat triangular surfaces and normal vectors for each of them. At this stage, mapping errors may occur. However, these errors can be minimized by adopting small modeling surfaces (Nee, Fuh & Miyazawa, 2001; Kowalska-Bany & Krokosz, 2008).

Then, in the STL model, contour lines, which are used to create the SLA model, are isolated (Fig. 1c, d). The SLA model is made of layers of a predetermined thickness. For example, for 3D Systems SLA-250, the thickness of the layers can be 0.1 or 0.15 mm, respectively.

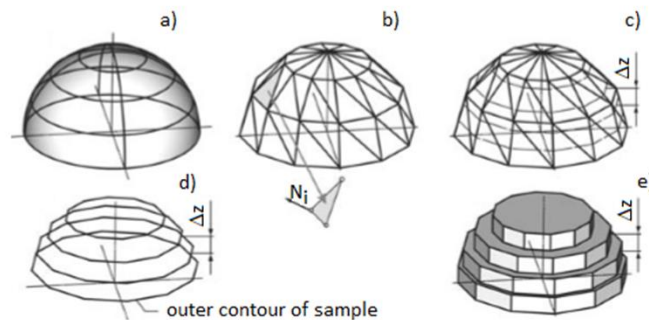


**Fig. 1. Stereolithographic model creation process: a) CAD model, b) STL model, c, d) division of STL model into layers, e) ready SLA model;  $\Delta z$  – thickness of single layer of SLA model,  $N_i$  – normal vector (Kowalska-Bany & Krokosz, 2008)**

The model is shaped on a working platform immersed in a photocurable resin. In the initial stage of model shaping, the first layer of the model is made. The platform is immersed in the resin to the depth of the assumed layer thickness of the model. The laser beam imitates the layer's outline in the resin and then hardens the area inside the overlapping stitches. After building each subsequent layer of the model, the platform is dipped again in the resin to the depth of the assumed layer thickness. The laser beam hardens the next layer of the model. The next model building sequences are similar to each other. The process continues until the entire model is mapped.

SLA technology was established as a cheaper alternative to other manufacturing methods for rapid prototyping. Its advantage is the ability to create models of complex internal and external construction, requiring high accuracy. For example, thanks to models made of a transparent resin, it is possible to create prototypes with a visible internal structure, which allows, for example, to examine traces of cooperation between gears or stresses.

In this work, photocurable resins were tested in a quasi static tensile test, then numerical analyzes were performed validating the material model selected for the resin. These studies will be used for further work, which will be analysis of porous structures with different void distributions.

## **2. EXPERIMENTAL TESTS**

Identification tests of mechanical properties of materials are aimed at determining the basic parameters and characteristics of selected materials to compare them and define a group of materials with the best properties. The obtained data will also allow to create constitutive models of the materials studied.

The tests were carried out for standard samples printed from two different materials: Tough resin and Clear resin. The stretching speed of 5mm/min to determine and compare their mechanical properties was applied.

### **2.1. Samples**

Standard samples for experimental research were made using rapid prototyping technology, which is 3D printing using the SLA method on the printer FormLabs 2. The first stage is to prepare the model in the PreForm software dedicated to the device, which allows you to adjust its quality (the layer height was 0.1 mm – the so-called quick print), the choice of material and the orientation of the element in the workspace. Supporting structures have been added automatically. The next step is the 3D printing process itself (Fig. 2). To ensure maximum repeatability, each process is carried out at a constant, regulated resin temperature. Such a procedure allows to reduce the viscosity of the photopolymer and to remove air bubbles from it.

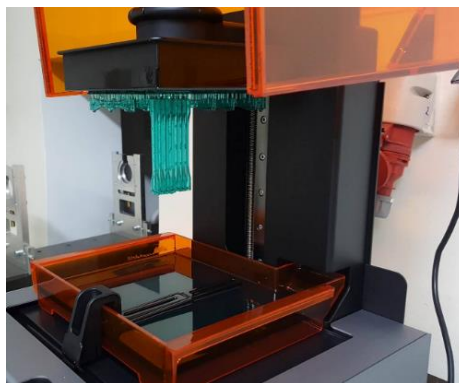


**Fig. 2. Printing in SLA technology before removing from work platform**

One of the most demanding activities for which time should be spent in 3D printing in SLA technology is post-processing. The first step is to remove the unbound resin from the model, usually both by bath in isopropanol. The next stage of cleaning the model is required due to the process characteristics. The use of a bathtub with resin forces the use of support structures from the native material, and their removal is done mechanically. To facilitate cleaning the model from the supports, the Form2 device uses a different scan style when building them – such structures have lower mechanical strength. This is usually done by tools that allow cutting, for example, pliers or knives.

After removing the support structures, the traces in which the slides joined the model remain. In order to increase the accuracy of the stereolithography method, the laser power is somewhat limited. Too much power would cause the resin to also harden around a focused laser spot. And this is the reason of applying the last, recommended step. It consists in the final hardening of the photopolymer in the UV chamber. The treatment allows to achieve maximum mechanical and chemical properties for a given material. It should be noted that depending on the size of the model as well as the material used, the time and power of exposure may vary. In addition, the samples after exposure were subjected to temperature in a chamber preheated to 60°C during 1h for the Clear resin and 2h for Tough resin.

## 2.2. Static tensile test

The presented test consists in axial tensile of the normalized sample until its destruction, with a constant traverse speed at room temperature.

During the test, the force necessary to extend the sample is recorded. On the basis of the obtained data it is possible to determine the basic stress-strain characteristics, which is the basic source of information on the mechanical properties of the material.

The forces and displacements obtained from the tests were converted into engineering stresses and strains according to the following relationships:

- engineering stress:

$$\sigma_{eng} = \frac{P}{A} \quad (1)$$

where:  $P$  – applied force,  
 $A$  – initial area of cross-section.

- engineering strain:

$$\varepsilon_{eng} = \frac{\Delta l}{l} \quad (2)$$

where:  $l$  – sample initial length,  
 $\Delta l$  – change in length.

Due to the fact that the constitutive models of materials in the LS-Dyna system require the application of real strain values, taking into account the change in the cross-section of the sample due to tensile, they were calculated from the equation:

$$\varepsilon_{real} = \ln(1 + \varepsilon_{eng}) \quad (3)$$

The conditions and the method of conducting the tensile testing of plastics are described in the PN-EN ISO 527-1 standard "Plastics. Determination of mechanical properties at static tension". The sample is flat and has the shape of a "paddles" (Fig. 3). The dimensions of the sample should be as follows: thickness  $4.0 \pm 0.2$  mm, width of the gauge length  $10 \pm 0.2$  mm and overall length over 150 mm. Table 1 presents all dimensions of the samples used in the tests.

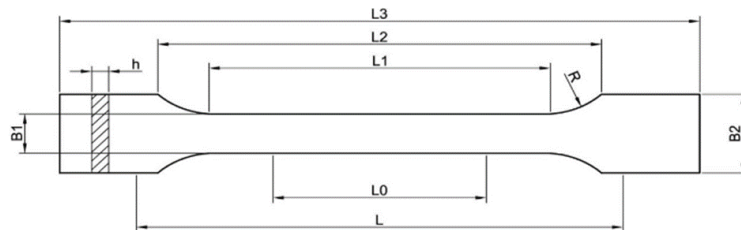


Fig. 3. Scheme of sample in accordance with PN-EN ISO 527 standard

Tab. 1. Characteristic dimensions of samples according to scheme shown in Fig. 3

Symbol	Dimensions [mm]
L1	$80 \pm 2$
L2	20 to 25
L3	150
R	104 to 113
B1	$10 \pm 0.2$
B2	$20 \pm 0.2$
H	$4.0 \pm 0.2$
L0	$5.0 \pm 0.5$
L	$115 \pm 1$

Samples were tensiled using a Zwick Roell Kappa 500 testing machine (Fig. 4) at room temperature of about  $20^{\circ}\text{C}$ . The stand was equipped in videoextenometer, which enabled a non-contact measurement of deformation of the sample in many axes and, thanks to special modules, measurement of the narrowest or widest place of the sample, angle of deflection, distribution of deformations in a given axis, measurement of XY coordinates of points on the plane. Dimensions of standard samples were proportionally reduced by appropriate cross-section scaling.

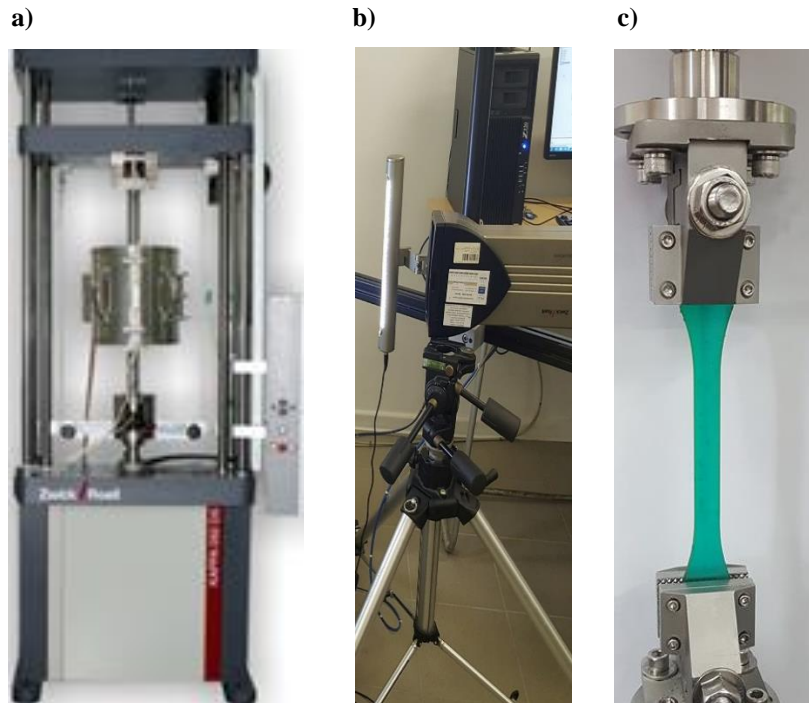


Fig. 4. View of a) Zwick Roell Kappa 500 machine, b) videoextensometer and c) sample placed in jaws of machine

### 2.3. Experimental tests results

On the basis of conducted experimental tests of uniaxial tensile, the force – displacement characteristics were obtained. Based on the equations (1) and (2), the engineering stress vs. engineering strain curves were determined for the 5mm/min load speed. They are summarized in Fig. 5 and 6.

Based on the curves obtained in the experiment, Young modulus, elongation at break and tensile strength were determined. The data were summarized in Table 2.

Tab. 2. Comparison of material data for Tough and Clear resin

Parameter	Tough resin	Clear resin
Young modulus	2495.72	2907.31
Elongation at break [%]	12.79	6.93
Tensile strength [MPa]	72.04	53.41

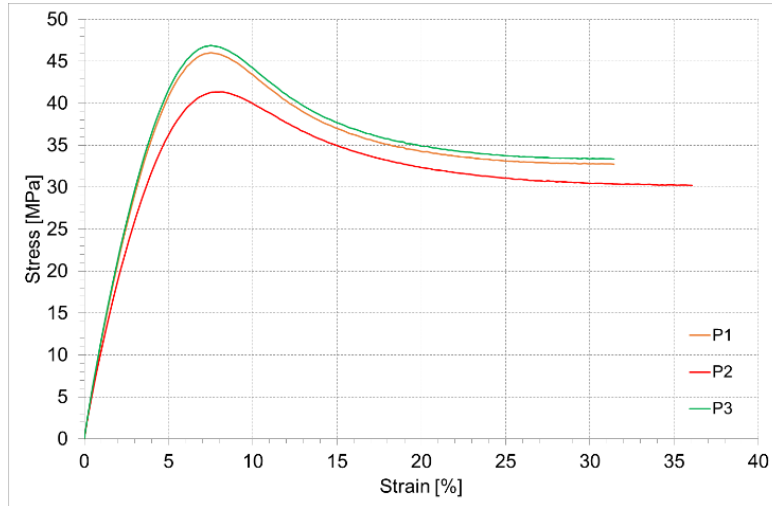


**Fig. 5. Engineering stress vs. engineering strain characteristics for tensile test of Tough resin**

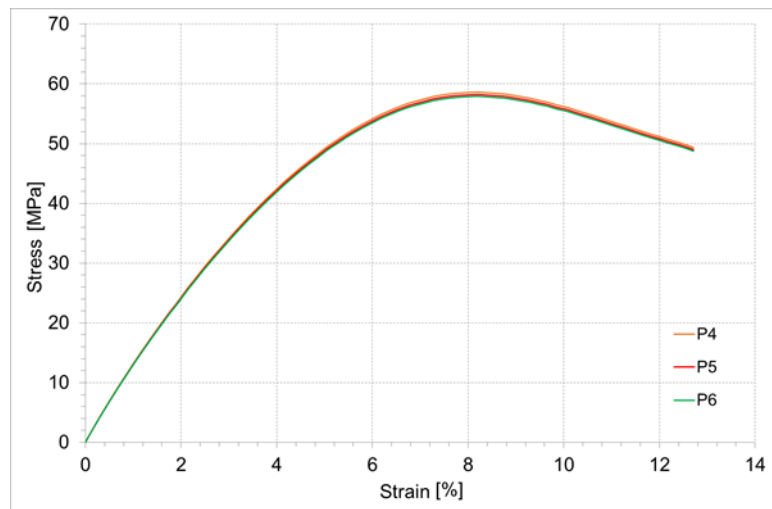


**Fig. 6. Engineering stress vs. engineering strain characteristics for tensile test of Clear resin**

Experimental research shows that the analyzed materials differ significantly in strength properties. Clear resin has high tensile strength, and low elongation at break. Tough resin, on the other hand, was designed like an ABS material and has better elastic properties and improved impact resistance, but lower Young modulus and tensile strength.

### 3. NUMERICAL ANALYSES

Simulation of quasi-static tensile was aimed at developing a numerical model of a photocurable resin material. The numerical model of the sample was shown in Fig. 7.



Fig. 7. Numerical model of a paddle sample

The model consisted of 5520 elements of the HEX8 type with the formulation of ELFORM 1. A rigid procedure for counteracting the F-B hourglass effect was used (IHQ = 4). The cross-section of the sample in the measuring area was  $5.4 \times 1.96$  mm.

#### 3.1. Material model selection

Due to the fact that the material will be used to simulate quasi-static compression of microstructural models, the basic elastic-plastic material MAT\_024 was selected.

MAT 024 is an elasto-plastic constitutive model based on von Mises yield criteria which is used to model the material behaviour until the point where instability occur. The input parameters implemented in the MAT 024 card are primarily Young modulus, the mass density, Poisson's ratio and the hardening of the material. The hardening curve shall only cover the loading path until instability initiates (Hallquist, 2006).

Furthermore, the model supports more complex material behaviour where the material is strain rate dependent, i.e. a visco-plastic model. Instead of implementing one hardening curve, a table defining different strain rates which are connected to a certain hardening curve has to be implemented to capture the behaviour. However, MAT 024's properties are not able to express the material behaviour beyond the point of uniform expansion.

Deviatoric stresses are determined that satisfy the yield function (Hallquist, 2006):

$$\phi = \frac{1}{2} S_{ij} S_{ij} - \frac{\sigma_y^2}{3} \leq 0 \quad (4)$$

where:

$$\sigma_y = \beta [\sigma_0 + f_h(\varepsilon_{eff}^P)] \quad (5)$$

and  $f_h(\varepsilon_{eff}^P)$  is the hardening function. The parameter  $\beta$  accounts for strain rate effects.

For complete generality a table defining the yield stress versus plastic strain may be defined for various levels of effective strain rate. In the implementation of this material model, the deviatoric stresses are updated elastically, the yield function is checked, and if it is satisfied the deviatoric stresses are accepted. If it is not, an increment in plastic strain is computed (Hallquist, 2006):

$$\Delta \varepsilon_{eff}^P = \frac{\left(\frac{3}{2} S_{ij}^* S_{ij}^*\right)^{1/2} - \sigma_y}{3G + E_p} \quad (6)$$

$G$  is the shear modulus and  $E_p$  is the current plastic hardening modulus. The trial deviatoric stress state  $S_{ij}^*$  is scaled back (Hallquist, 2006):

$$S_{ij}^{n+1} = \frac{\sigma_y}{\left(\frac{3}{2} S_{ij}^* S_{ij}^*\right)^{1/2}} S_{ij}^* \quad (7)$$

Material parameters were adopted from the experimental studies presented above. Parameter responsible for damage – effective plastic strain were calculated from formula (3). For Tough resin, it was 1.153, for Clear resin – 0.67.

### 3.2. Numerical calculations results

Exemplary model deformations for Tough resin and stress – strain chart were shown in Fig. 8, for Clear resin – in Fig. 9,

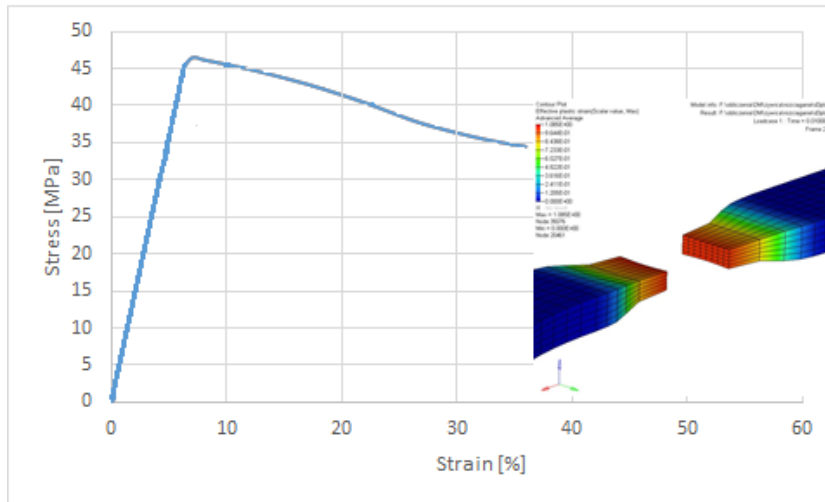


Fig. 8. Deformations and stress-strain chart for Tough resin model

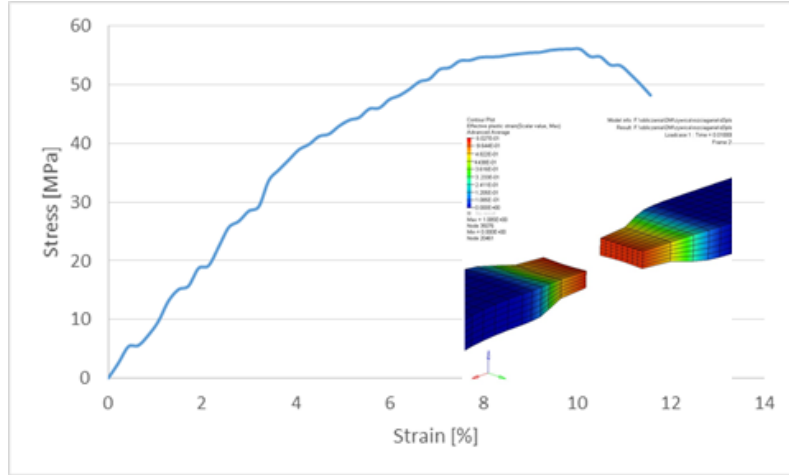


Fig. 9. Deformations and stress-strain chart for Clear resin model

#### 4. DISCUSSION

The results of numerical and experimental tests were compared in Fig. 10.

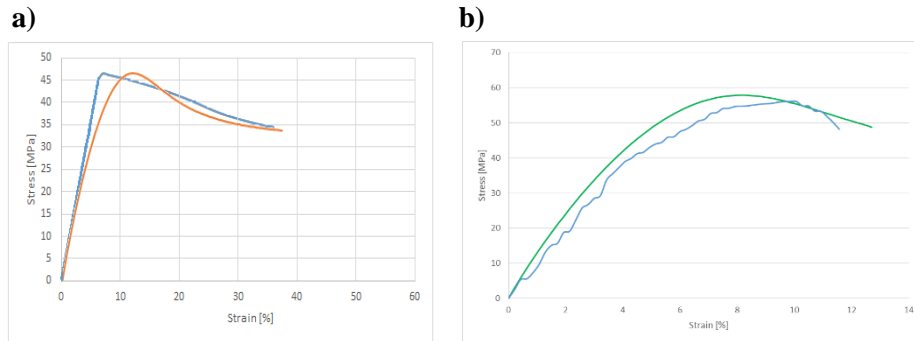


Fig. 10. Comparison of experimental and numerical tensile tests for:  
a) Tough resin, b) Clear resin

The relative error for the proposed material model was calculated as the quotient of the absolute error and the exact value  $x_0$ :

$$\delta_x = \frac{\sum_{i=1}^n \frac{\Delta x}{x_0}}{n} = \frac{\sum_{i=1}^n \left( \frac{x-x_0}{x_0} \right)}{n} \quad (8)$$

where:  $x$  – measured value,  
 $\Delta x$  – absolute error,  
 $n$  – number of measuring points.

This error for the Tough resin was 12.1% for the Clear resin – 18.7 %.

After the analysis, it can be concluded that the choice of material constants is correct. Errors in numerical analysis result from simplifications of the introduced model of elastic-plastic material.

The numerical tensile test of the sample in a qualitative and quantitative manner corresponds to the real phenomenon.

#### ACKNOWLEDGEMENTS

*The research presented in the paper was supported by grant No BG2/DIOX4SHELL/14 titled “Development of guidelines for design of innovative technology of shale gas recovery with the use of liquid CO<sub>2</sub> on the base of numerical and experimental research – DIOX4SHELL”, supported by the National Centre for Research and Development (NCBR) in years 2014–2018.*

#### REFERENCES

- Attaran, M. (2017). The rise of 3-D printing: The advantages of additive manufacturing over traditional manufacturing. *Business Horizons*, 60(5), 677–688.
- Hallquist, J. O. (2006). *LS-DYNA Theory Manual*. Livermore Software Technology Corporation.
- ISO/ASTM International Standard. (2015) *Additive manufacturing – General Principles – Overview of process categories and feedstock* (17296-2:2015(E)).
- Kowalska-Bany, K., & Krokosz, J. (2008). Rapid Prototyping – Historical Overview. *Odlewnictwo współczesne – Polska i Świat*, 112–118.
- Melchels, F. P. W., Feijena, J., & Grijpmaab, D. W. (2010). A Review on Stereolithography and Its Applications in Biomedical Engineering. *Biomaterials*, 31, 6121–6130.
- Nee, A. Y. C., & Fuh, J. Y. H., & Miyazawa, T. (2001). On the improvement of the stereolithography (SL) process. *Journal of Materials Processing Technology*, 113(1–3), 262–268.